Journal of Sol-Gel Science and Technology (2021) 97:638–650
https://doi.org/10.1007/s10971-021-05468-3

ORIGINAL PAPER: SOL-GEL AND HYBRID MATERIALS FOR CATALYTIC, PHOTOELECTROCHEMICAL AND SENSOR APPLICATIONS

Polymer surfactant (Triton-100) assisted low cost method for preparing silver and graphene oxide modified Bi-MnO_x nanocomposite for enhanced sensor and anti-microbial health care applications

Jothi Ramalingam Rajabathar[1] · Prabhakarn Arunachalam[1] · Hamad A. AL-Lohedan[2] · Radhika Thankappan[3] · Jimmy Nelson Appaturi[4] · Thiruchelvi Pulingam[5] · Wasmiah Mohammed Dahan[1]

Received: 7 October 2020 / Accepted: 2 January 2021 / Published online: 4 February 2021

Abstract

Silver nanoparticles decorated on nanotubes morphology of Bismuth doped manganese oxide (Bi-MnOx) was prepared by Triton-X-100 polymer assisted precipitation process. In the second step, Ag nanoparticle with very fine particle size and graphene nanoparticle deposition by high power ultra-sonication method. Biogenic route synthesized silver nanoparticles have forms the spherical particle morphology with particle size obtained <10 nm. Polymer assisted method prepared pristine Bi-MnOx has existing in Nano- tubular morphology. The nanotube formation/nano particle incorporation has clearly confirmed by Scanning and Transmision electron microgph images. The synthesized silver nanoparticle modified Bi-MnO_x composite was further tested for non-enzymatic detection of hydrogen peroxide sensor application. To exploit the biological activity of as prepared Bi-MnOx and biogenic route prepared silver quantum dot (QDs) particle and graphene oxide (GO) modified Bi-MnOx nanocomposite was further studied for gram positive and gram-negative bacterial strain. The nanoparticle dispersed Bi-MnOx could be adopted as low cost coating materials in health care smart building construction. Diffuse reflectance spectral studies are described for as prepared Ag QDs/GO doped Bi-MnOx is shown reduced band gap values (2.93 eV) than the pristine Bi-MnOx (3.17 eV) and it could be adopted for visible light photo-catalysis and antimicrobial applications.

Graphical Abstract

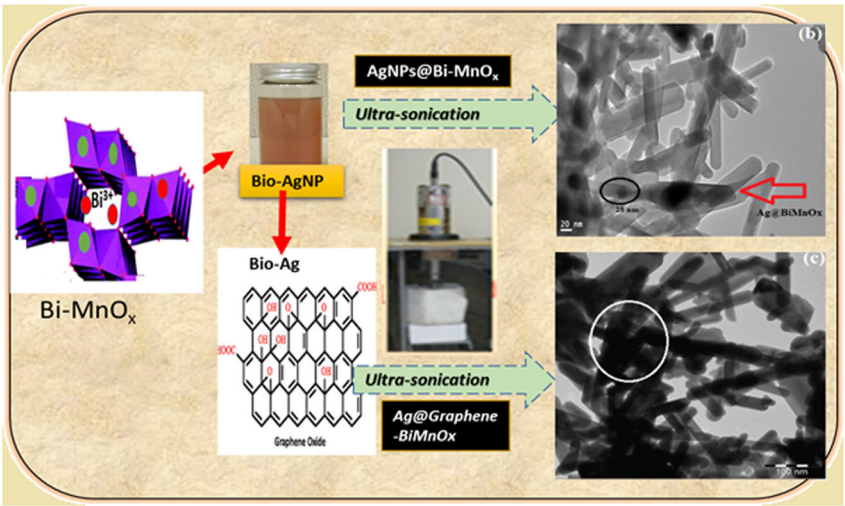

✉ Jothi Ramalingam Rajabathar
jrajabathar@ksu.edu.sa

Extended author information available on the last page of the article

Keywords Bismuth oxide · Manganese oxide · Nanotube · Silver nanoparticles · H_2O_2 · TritonX-100

Highlights

- Silver nanoparticles with quantum dot particles are produced by the biogenic route.
- Ag QDs incorporated on Bi- MnOx nanotubes show effective porous texture.
- Ag QD and GO are inserted into the tubular morphology of Bi-MnOx.
- Ag@Bi-MnOx and Bi-MnOx show effective antibacterial activity.
- Ag@Bi-MnOx and Ag-Bi-MnOx/GO show promising sensor activity.

1 Introduction

Nanostructures of porous manganese oxide based composite material have studied in the past decades for catalytic and electrochemical applications such as non-enzymatic sensors, cathode materials in battery application and in supercapcitor device fabrication [1–6]. Different types of metal ion doped porous manganese oxide and silver nanoparticle modified manganese oxide material have also been exploited in the field of catalytic oxidation reactions, removal of heavy metal ions and antibacterial activity application [7–11]. In recent years, many preparation strategies have exploited to synthesis porous and mesoporous manganese oxide and nanoparticle incorporated manganese oxide for water oxidation toward renewable energy application and super capacitor application [12–15]. Manganese oxides (MnOx) or MnO_2 has been extensively investigated due to variety of crystallographic forms (α, β, γ, and δ), low cost, and high theoretical Cs (1370 F g^{-1}) [3, 16, 17]. In spite of being a very good pseudo capacitive material, commercial application of manganese oxide (MnO_2) is limited due to its low electrical conductivity, structural instability and low rate capability [3, 14]. Therefore, to fabricate a composite form of with metal ion modified manganese oxide could be more potential candidate to overcome the disadvantages of bulk MnO_2. In this regard, a composite with graphene oxide, carbon nanotube (CNT) varieties such as single wall and multi wall (MWCNT) type carbon nanomaterial is preferred to disperse into pseudo capacitive manganese oxide, could provide good conductivity and entangled hybrid micro and mesoporous structure for manganese oxide based composite materials [18–20]. Insitu doping of metal ion into the manganese oxide octahedral structure results in the formation improved average oxidation state and provide efficient redox property [18]. Bismuth oxide supported manganese oxide catalyst preparation for nitrous oxide from ammonia was reported by Ivanova et al. [21]. They prepared Mn–Bi–O-supported catalysts using incipient wetness impregnation for the catalytic production of nitrous oxide using different weight percentage loading of Bi_2O_3 on MnOx matrix. The conversion of methane to fuels is a important catalytic technological challange and Baidikova et al. [22] reported bismuth-manganese oxide catalysts for methane oxidative coupling. The oxides of group II and oxides of rare earth metal combination promoted with alkali metal are most intensively studied catalytic materials in the past [21, 22]. Apart from catalytic study, Bismuth oxide coated amorphous manganese oxide materials have also recently reported for electrochemical super-capacitor application. The bismuth containing compounds have used as the additives for the metal ion modified layered MnO_2 electrodes in the rechargeable batteries, as the doping of bismuth to MnO_2 could increase its charge-discharge characteristics and improve the cycle-stability [23]. The results are showing that 5 wt.% Bi_2O_3 is coated on the amorphous MnO_2 provide the specific capacitance value of 352.8 F/g [24]. In another related study, redox mediated synthesis of hierarchical Bi_2O_3/MnO_2 fabricated for development of non-enzymatic hydrogen peroxide electrochemical sensor study [25]. Mamatha et al. reported bismuth modified strontium containing perovskite materials for electromagnetic applications [26]. It is interesting to note that the Bismuth doping creates the large magneto caloric effect for the resultant perovskite compounds. In terms of chemical property, Bi^{3+} is highly polarized in certain Bi-O bond direction and it can increase the average oxidation state of manganese exist in the porous octahedral tunnel structures [27]. Jothi Ramalingam et al., reported silver nanoparticle modified undoped mesoporous texture of manganese oxide for enhanced antibacterial and anti-cancer activity for health care applications [28]. The sonochemical assisted deposition method has not been employed in the formation of Ag QDs/GO incorporation on porous Bismuth-doped MnO_x nanotube fabrication. Therefore, in the present study, silver and graphene oxide nanoparticles have incorporated by ultrasonication method into the nanotube structure of Bi-MnOx. The as-prepared materials have studied comparatively, with respect to their activity for hydrogen peroxide sensor and antibacterial activity. Finally, the physicochemical, surface textural and morphological properties of the as-prepared nanocomposites materials have also demonstrated.

2 Materials and methods

2.1 Materials

Silver nitrate ($AgNO_3$) manganese sulfate ($MnSO_4$), bismuth nitrate ($Bi(NO_3)_3$), non-ionic surfactant (Triton X-100), potassium persulfate ($K_2S_2O_8$), ammonia and all other chemicals have purchased from Sigma Aldrich and used without further purification. The detailed characterization study of the prepared composite materials were carry out by X-ray diffraction, scanning electron microscopy transmission electron microscope, and N_2-sorption isotherms analysis. The ultra-sonication is carry out by Sonicator (Branson Digital Sonifier-400) for the deposition process. Diffuse reflectance spectra (DRS) and band gap energy calculation were demonstrated by kubelka-munk method using Shimadzu UV-2600 spectrophotometer.

2.2 Synthesis of Bi-MnOx and silver nanoparticle/graphene oxide deposition composites

The Bi-MnOx is prepared by precipitation procedure by taking a 2:1 ratio of manganese sulfate to bismuth nitrate substance and both mixed in water and stirred continuously to dissolve inorganic salts (1). Similarly, in another beaker, the required quantity (mL) of Trixton-100 was mixed with 500 ml of water (2). The sodium persulphate (45 g in 50 mL), was added dropwise to the above-mixed solution and then added 80 mL of aqueous ammonia solution. The above-mixed solution was continued to stir at least 12–13 h followed by filtration and dry the brown solid at 110 °C to remove the volatile matters. The resultant solid was calcined at 400 °C for 3 h to form mesoporous Bi-MnOx. The above route prepared 1 g quantity of Bi-MnOx is dried and calcined at 400 °C for 3 h, after the complete removal of the surfactant. Plant extract (extract of *Alternanthera Bettzickiana)* route prepared biogenic Ag QD (10 mg) Nanoparticles is dispersed by wet impregnation technique on porous Bi-MnOx. The detailed preparation of silver nanoparticle was descripted by our previous report [28]. The required quantity of solid Bi-MnO_x is mixed with deionized water followed by 15 min of ultra-sonication. For the preparation of Ag@GO-Bi-MnOx composite, 1 g of Bi-MnOx mixed with 200 miligrams of commercial graphene oxide followed by ultra-sonicated for 15 min. In the second step, addition of 10 mg Silver QD nanoparticles on GO-Bi-MnOx for dispersion process to fabricate Ag@GO-Bi-MnOx. The material prepared by the above method is designated as 1wt %Ag-BiMnOx and 1wt %Ag-GO-BiMnOx.

2.3 Electrochemical characterization study

The required qunatity (5 µL) of silver/GO nanoparticle deposited Bi-MnOx dropped on glassy carbon electrode followed by dried in air. In the next step is to add the 2 µL quantity of nafion solutions on top of modifed GCE electrode to fabricate modified electrodes. The similar way Graphene oxide mixed with Bi-MnOx followed by ultra-sonicated for 5 min. The as-prepared GO-Bi-MnOx further deposited with Silver nanoparticle in the ultra-sonicated process to form the paste. The paste is dropped on cleaned Glassy carbon electrode (GCE). The as-prepared modified electrodes were immersed in water to wet the nafion layer before usage.

The cyclic voltammetry studies of the as-prepared sample coated on GCE were investigated in phosphate buffer solution (PBS) at pH 7 for H_2O_2 sensor analysis. The reference electrode, a saturated calomel electrode (SCE), and a counter electrode (platinum foil) were used to study the electrochemical activity.

2.4 Band gap determination from diffuse reflectance spectra analysis

To calculate band gap from DRS data, hv is Energy F(r)hv is kubelka munk function times energy. The standard equation is $(F(r)hv)^{1/n} = A(Eg\text{-}hv)$. The plot $h\nu$ on x-axis and $F(r)(h\nu)^2$ on y axis could provide the information about band gap values of the respective sample.

2.5 Determination of antibacterial activity

Agar well diffusion method has used to determine the antibacterial activity. Mueller-Hinton agar plates were prepared and bacterial strain cultures by spread plate method using a sterile swab. In each plate, seven wells have made using a sterile borer. To well number 1 and 2, 100 µL of plant crude extract and 50 µL (50 µg) of $AgSO_4$ solution has added. Various concentrations of green synthesized AgNPs, were added into other wells. After incubation at 35 °C for 1 day, the diameter of the inhibitory zones around the wells in each plate has measured in millimeters.

3 Results and discussion

3.1 Physico-chemical characterization of AgNPs modified Bi-MnO_X composites

Figure 1 shows the schematic formation of undoped Bi-MnOx and silver QD size of nanoparticle and graphene oxide incorporation by the sono-chemical process for the

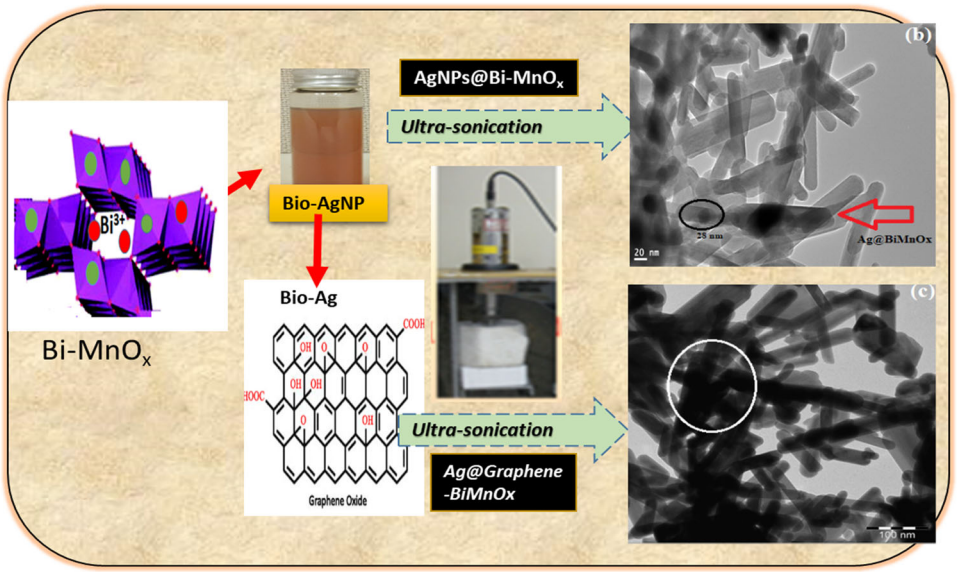

Fig. 1 Schematic of Low cost method prepared Bi-MnOx nanotube and silver quantum dot and graphene oxide incorporation by green chemistry (sonolysis) method

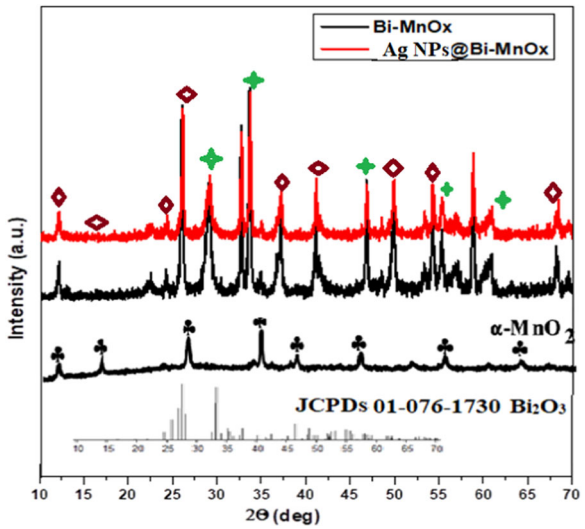

Fig. 2 Comparative XRD of Bi-MnOx- Nanotube and Silver (Ag) nanoparticle QD (Quantum dots) modified Bi-MnOx nanotubes. (and) α-MnO_2; Bi_2O_3

formation of Ag@BiMnOx and Ag-GO@Bi-MnOx nanotube composite formations. The QDs of individual silver nanoparticle prepared by biological reduction method was determined by XRD, particle size, TEM analysis [29, 30]. The nanoparticle formation is first confirmed by the XRD method before it deposits into the $BiMnO_X$ nanotube composite.

Figure 2 shows the X-ray diffraction pattern of Ag@Bi-MnOx and pristine Bi-MnOx, the crystalline phase formation is determined by comparing the JCPDS data of tunnel structured manganese oxide phases and respective bismuth oxide phases [31]. The d-space values and intense peaks obtained for the pristine B-MnOx and silver and graphene oxide modified nanotube composite matched very well with α-MnO_2 phase (JCPDS 42–1348), which is porous tunnel structure manganese oxide inter-connected with MnO_6 octahedrons. The major intense peak related with Bi_2O_3 are matched with the JCPDS card number-01-076-1730 [32]. In the present method, Bismuth ions are incorporated insitu to the framework of MnO_6 octahedran and it substitute in the framework position as well as internal porous structure of manganese oxide [23, 33]. There is no much difference observed in the XRD patterns of silver and GO modified Bi-MnOx composite due to its lower loading in Bismuth doped manganese oxide phase. At the same time, bismuth and carbon from graphene oxide content is confirmed by TEM-EDX analysis, which is discussed in detail in the below sections.

Figure 3 (a–b) shows the UV-Vis specta and XRD of AgNPs synthesized by the plant extract are good crystalline in nature. First the formation of silver nanoparticle from plant extract is confirmed by UV-Vis analysis, which is shown in Fig. 3a. The respective absorption spectra at 430 nm confirms the formation silver nanoparticles. The particle size of silver NPs was calculated using Debye-Scherer's equation $\{D = 0.9\lambda/\beta\cos\theta\}$ as well as by particle size analyzer. The crystallite size of AgNPs was calculated using the above formula by utilizing the most intense peak *hkl* value of (111) in Fig. 3b. The nitrate source prepared from silver nanoparticle is utilized to incorporate on Bi-MnOx matrix. In the coming sections demonstrate the comparative structural morphology and electro catalytic activity were evaluated for silver and GO nanoparticles modified bismuth doped porous manganese oxide (Bi-MnO_x) nanocomposites. The HR-TEM images are indicating that the occurrence of a very fine nanoparticle with QDs size is confirmed in the comming sections. The spherical shaped nucleation of the silver particle on top and inside of nanotubes of the

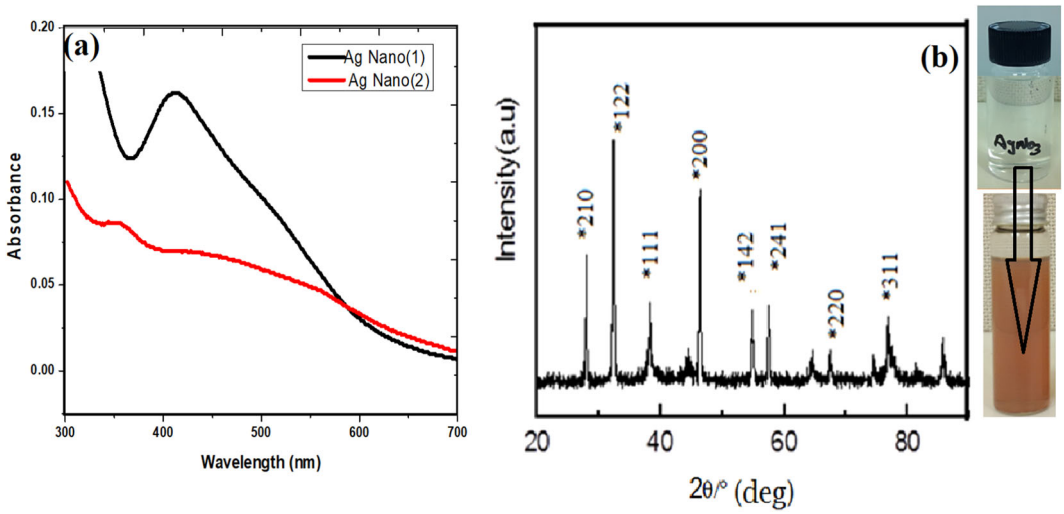

Fig. 3 UV-Vis spectra of prepared Silver nanoparticle (**a**) Silver nitrate source (1) and Silver sulfate sources (2) (**b**) XRD patterns Ag nanoparticle prepared by biogenic method using plant extract of *Alternanthera Bettzickiana*

individual tube morphology of bismuth doped manganese oxide have obtained by HR-TEM analysis [23, 33].

Figure 4 shows the Nitrogen adsorption and desorption nature of the non-ionic surfactant method prepared Bismuth doped manganese oxide (Bi-MnO_X) and Ag-Bi-MnOx composite. The respective pore size value and surface area of value are measured by reported method. The obtained N_2 sorption–desorption isotherm shapes are similar to H2-type hysteresis and type-IV (Fig. 4), with low relative pressure of 0.4–0.9 for the hysteresis loop, which is indicating the presence of ink bottle pores with narrow necks together with the thicker wall [34]. It contains both hybrid pore structure (micro as well as mesoporous) with an average pore volume and a total pore volume of 2×10^{-2} cc/g. The improved surface area value of (55 m^2/g) was obtained for Bi-MnOx. The similar Nitrogen adsorption and desorption measurement observed for Ag nanoparticles deposited composite with reduced pore volume after the deposition of silver nanoparticles in the internal matrix of Bi-MnOx. The inset of Fig. 4 shows the pore volume nature of as prepared composites, and the total pore volume of 8.9×10^{-3} cc/g and pores smaller than 15.7 A (radius) or 1.5 nm pore radiu was obtained (Fig. 4).

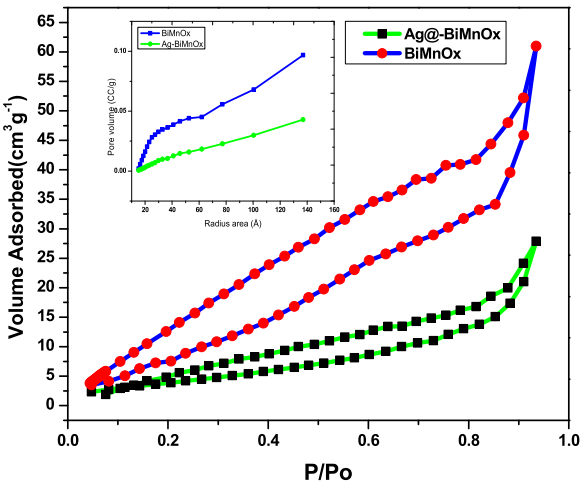

Fig. 4 Nitrogen adsorption desorption and pore size distribution of Bismuth doped MnO_x and silver nanoparticle incorporated Bismuth doped manganese oxide.

3.2 Structure and morphology characterization study

Figure 5 (a–d) shows the comparison study of SEM images of pristine Bi-MnOx and Ag (nano) incorporated Bi-MnOx nanocomposite materials. The pristine Bi-MnOx is showing spherical aggregated particle morphology with small needles at 2 and 5 µm exist inside the spherical shapes (Figs. 5a, c). In the case of silver doped Bi-MnOx shown in Fig. 6b, d (at a magnification of 1 µm and 0.5 µm) Ag is mostly existed as fine nanoparticle and this can be further confirmed with the results of high-resolution Transmission electron microscopy. The marked red lines in the picture represent the nanorods with particle size measurement of the prepared composite and it obtained particle size of 37 nm nanotubes for Bi-MnOx and after dispersion of silver nanoparticle provides the aggregated particle morphology with spherical particle size of 60 nm.

Figure 6 (a, b) shows High Resolution(HR)-TEM images of the pristine Bi-MnOx nanotube without silver or graphene oxide dispersion at 20 nm scale by high-resolution micrographs. HR- TEM analysis provides the fascinating nanotube shape for the as prepared bismuth doped MnOx materials with scale range of 20–100 nm size of nanotubes. Figure 6c, d shows the impact of glassy morphology

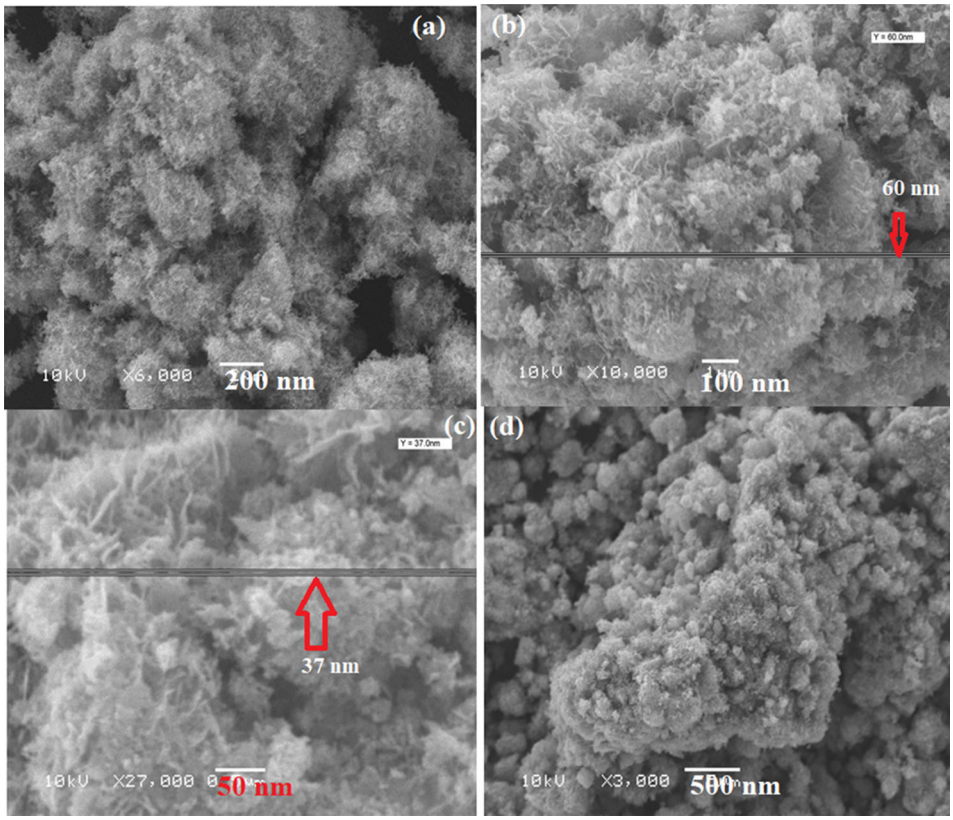

Fig. 5 **a and c** SEM images of Bi-MnOx Nanotubes and (**b & d**) Ag doped Bi-MnOx nanotube composite

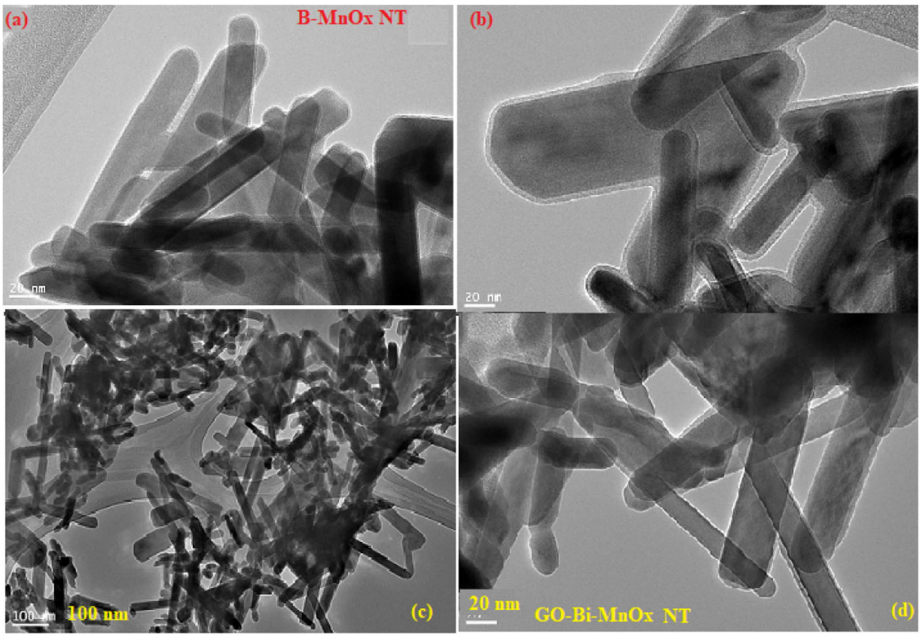

Fig. 6 TEM images of Porous Bi-MnOx nanotubes at various magnification (**a**–**b**) 20 nm scale; (**c**–**d**) Graphene oxide dispersed Bi-MnOx nanotubes at 100 nm and 20 nm scale

Graphene oxide insertion into the tubler structure of Bi-MnOx after the composite formation by ultrasoinic tratment. In the present method, the ultra-sonication process influence the reduced graphene oxide formation and exfoliated the nanotube morphology of Bi-MnOx. Figure 6c shows the darkish dispersion of reduced graphene oxide on

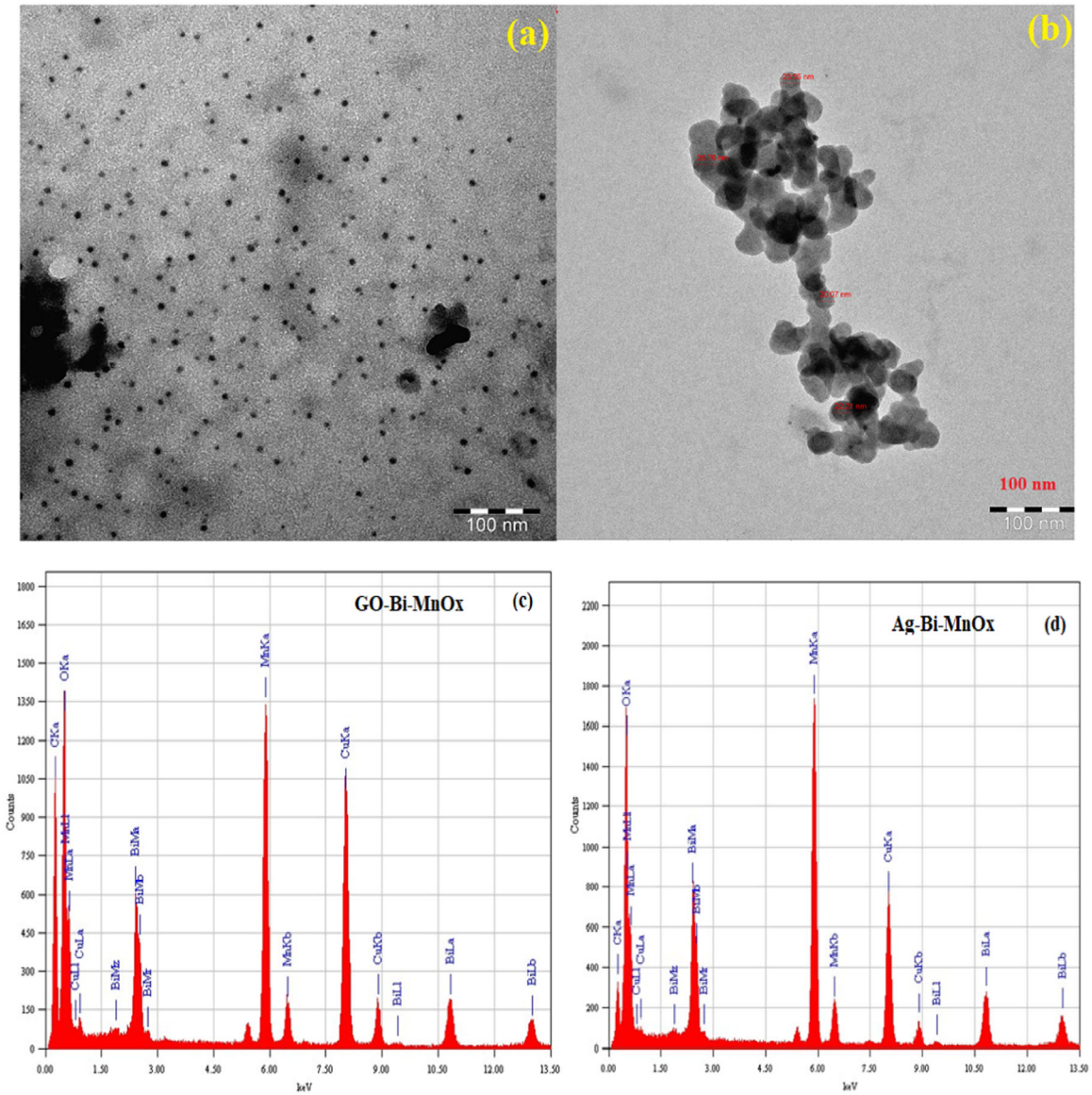

Fig. 7 (**a**, **b**) TEM Images of biogenic method prepared silver nanoparticle Quantum dots. (**c**) EDX spectra of GO@Bi-MnOx nanotube and (**d**) EDX spectra of modified Ag@ Bi-MnOx nanotube

manganese oxide matrix. Figure 6d showing the high-resolution image of graphene oxide incorporation inside the tubular structure of Bi-MnOx.

Figure 7 (a, b) displayed the individual silver quantum dot nanoparticles formation and particle aggregation shown at 100 nm scale range. Very fine nanoparticle shown as black dots in the in image are due to individual silver quantum dots with size ranges obtained below 10 nm. Figure 7(c, d) shows the elemental composition of Bi-MnOx nanocomposite after modification with silver and graphene oxide additives. The EDX data shown in Fig. 7 (c, d) for GO modified Bi-MnOx and it has shown the higher wt% loading of carbon with peaks obtained at 0.75 eV compared to Silver nanoparticle modified Bi-MnOx composite. The EDX analysis further confirms the presence of Bismuth and Manganese oxide formation at 1:2 wt% ratio in the final form of composite.

Our Biogenic method prepared silver nanoparticle shows very effective smaller nanoparticle size compared to other reported method of biogenic silver nanoparticle [32–35]. The reduction in the size of the particle could be potential for sensing activity towards trace level concentration detection in the electrochemical analysis [34, 35]. Hence, the as-prepared silver nanoparticle and Ag@graphene oxide-Bi-MnOx decorated composite has further applied in chemical sensor and antimicrobial applications.

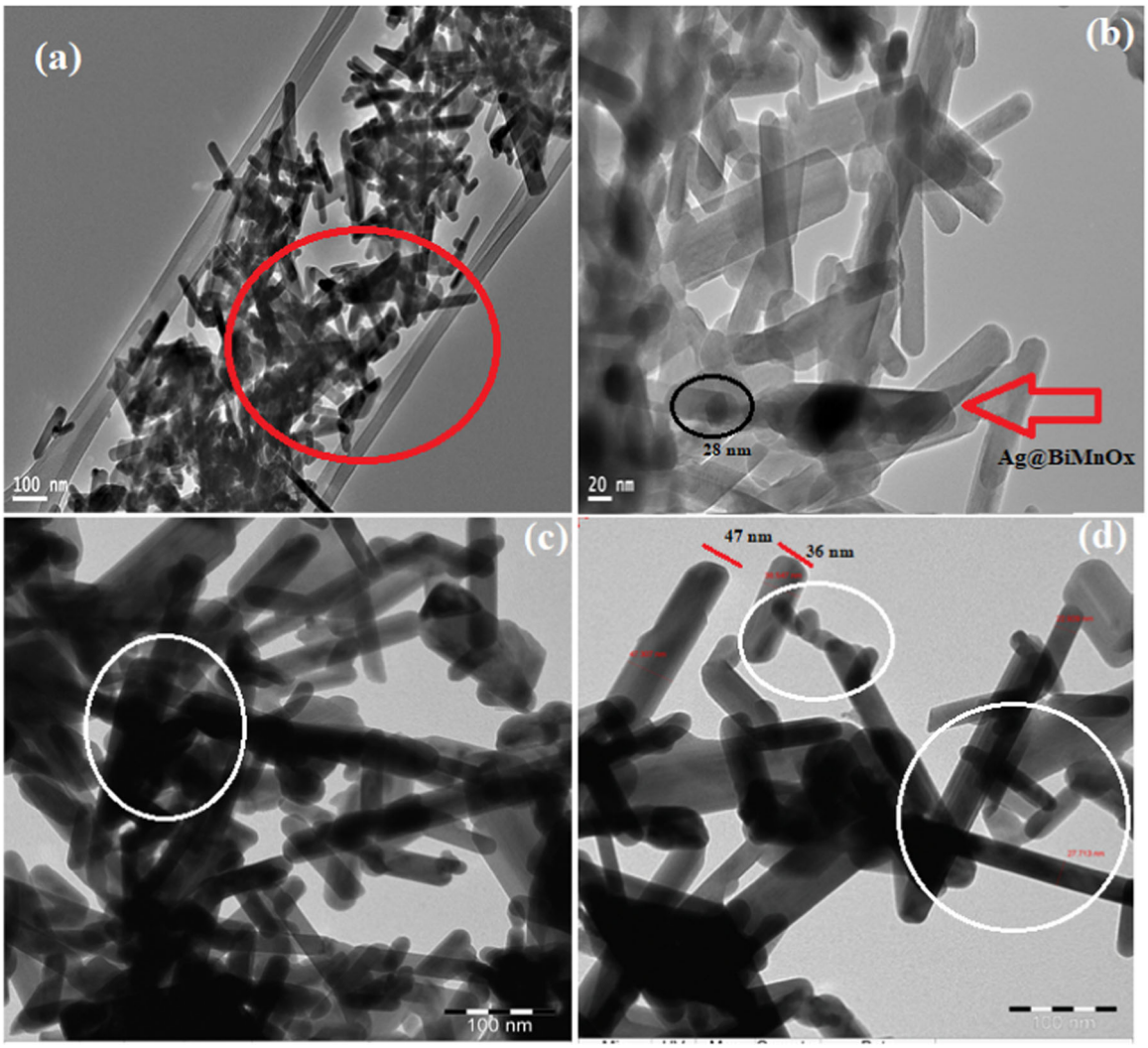

Fig. 8 HR-TEM of Ag@ Bi-MnOx nanocomposite at (**a**) 100 nm (**b**) 20 nm; Ag/graphene oxide@BiMnOx (**c**) 100 nm; (**d**) 100 nm

Figure 8(a, b) shows the TEM images shows the tiny nanotube morphology for Bi-MnOx and silver particle exist as Quantum dot size (black circled in Fig. 8b). Silver nanoparticles with metallic nature look like dark blackish with spherical shapes particle has inserted in nanotube morphology in Fig. 8a, b. Figure 8c is showing the higher resolution magnified images of Ag-GO@ Bi-MnOx nanotube, which is marked as white line and blackish rods deposition due to silver nanoparticle and reduced graphene oxide (r-GO) anchoring on porous morphology of tubular structure Bismuth doped manganese oxide. Due to ultrasonic action in strong dispersion of graphene oxide and silver QDs nanoparticle causes effective dispersion and incorporation into tubular structure of Bi-MnOx (white circles) in Fig. 8d, compared to empty nanotube morphology of pristine Bi-MnOx (Fig. 8). TEM images are clearly confirming the nanotubes morphology formation by insitu addition of Bismuth is playing key role in tubler morphology formation and it further confirms the graphene oxide and silver QDs insertion into the nano tubler structure of Bi-MnOx.

3.3 Electrochemical sensor and antibmicrobial study

The silver modified metal ion undoped pure mesoporous manganese oxide deposited with graphene oxide materials were already studied for pollutant removal application by our group [28]. In the present study, the ultra-sonication deposition method prepared Ag quantum dots of size below 10 nm by bio-reduction method followed by deposited on bismuth-doped porous manganese oxide to test the electrochemical sensing nature of the same. Figure 9 (a, b) are showing electrochemical sensing activity towards hydrogen peroxide concentration effect for porous Ag@$BiMnO_x$

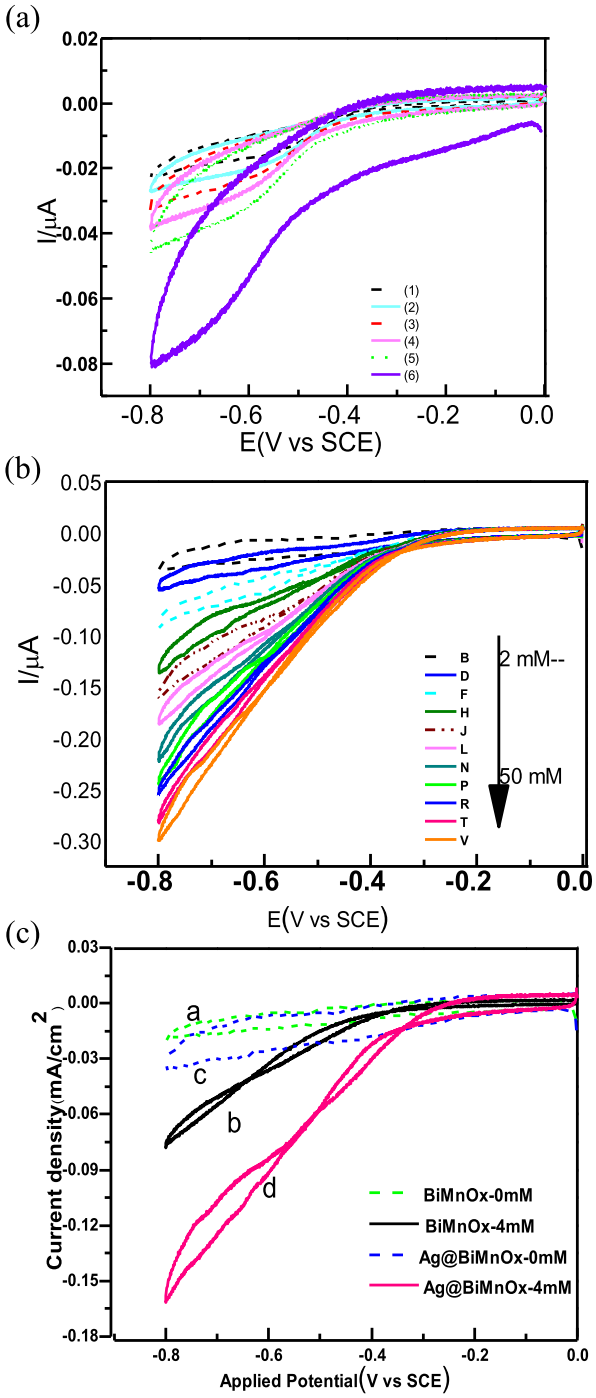

Fig. 9 **a** Cyclic voltammetry behavior of bare GCE (1), commercial MnO_2 (2); porous Bi-MnOx (3) Ag nano/MnO_x (4) 1%Ag nano loaded Bi-MnOx (5) 1% Ag-Graphene oxide/Bi-MnOx (6) in the presence of 2.5 mM H_2O_2 in phosphate buffer solution (NaH_2PO_4) at pH 7 and scan rate of 50 mV s^{-1}. **b** cyclic voltammetry analysis on Ag-Bi-MnOx modified GC electrode behavior in the presence of various concentration (2–50 mM H_2O_2) in phosphate buffer (PBS) solution at pH = 7. **c** Concentration effect of hydrogen peroxide on Bi-MnO_x and Ag-BiMnO_x modified electrode

modified GC electrode. The electrochemical activity of the non-enzymatic sensor analysis on Ag@BiMnO_x modified electrode is shown in Fig. 9a. The bare GCE and commercial MnO_2 showing poor activity than BiMnOx modified electrode and silver and graphene oxide deposited Bi-MnOx shows improved current density values. Figure 9a indicating Ag nanoparticle modified Bi-MnOx has a higher sensitivity response and higher current density values compared to undoped Bi-MnOx. Figure 9b shows the different concentration of hydrogen peroxide addition on Ag@BiMnOx for its sensing activity, upon increase in concentration from 2 mM to 50 mM showing gradual increase of current density. The plot of linearity follows the straight line for the sensor activity. Figure 9c shows the comparative cyclic voltammogram plot of electrochemical sensing activity of as-prepared pristine Bi-MnOx and biogenic silver nanoparticle deposited Bi-MnOx modified GCE at two different concentration such as in the absence and 4 mM concentrations of hydrogen peroxide addition in the presence of phosphate buffer solution (pH = 7). The 4 mM solution of hydrogen peroxide showing enhanced current response on Bi-MnOx modified GC electrode for H_2O_2 detection and it further enhanced by silver nanoparticle incorporated Bi-MnOx nanocomposite, which is shown in Fig. 9c. The addition of nanoparticle in the matrix of Bi-manganese oxide could facilitate the electron transport between electrode surface and solution interface [35]. Hence, the as-prepared silver modified Bi-MnOx nanocomposite electrodes could provide the site-selective electro-catalysis and specific bio-sensing of drug molecule analysis in future studies.

3.4 Band gap characterization and antimicrobial activity of as prepared modified Bi-MnOx composite materials

Figure 10a shows the diffuse reflectance UV-Visible spectra of Bi-MnOx and Ag nanoparticle modified Bi-MnOx nanotube in solid-state mode has analyzed to determine the band gap values. Band gap values from DRS in UV-Visible mode could provide the information about visible light sensing activity of the respective semiconductor metal oxide samples. DRS peaks of Bi-MnOx nanotube shows two linear reflectance at 370 nm and another one at 423 nm linearly. After deposition of silver quantum dot deposition on nanotube morphology of Bi-MnOx shows distorted DRS peaks at 420 nm and another linear reflectance peak at 370 nm. Further, Kubelka-Munk method [36] is adopted to derive the respective band gap alteration was calculated between nanoparticle doped and un-doped Bi-MnOx. Figure 10b shows the clear evidence of alteration in band gap structure of Ag-Bi-MnOx and Bi-MnOx in terms of binding energy values. After silver quantum dot deposition in nanotube structure of Bi-MnOx reduces the energy levels and band gap values from 3.17 eV to 2.93 eV and it

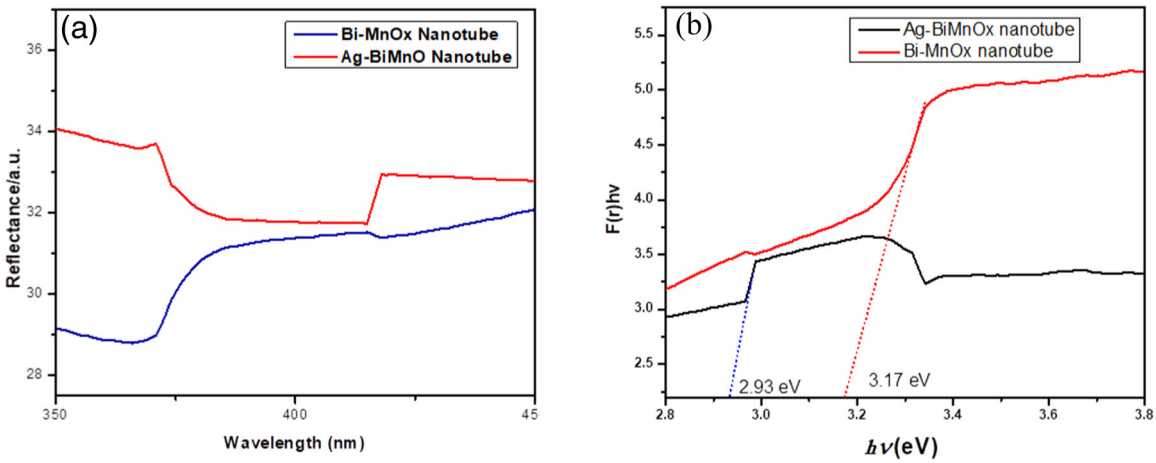

Fig. 10 **a** Diffuse Reflectance Spectra of pristine and silver nanoparticle modifed Bi-MnOx nanotube (**b**) K-M Function based band gap energy determination

enhances the redox electron transport for adsorption reactions [25]. Hence, it indirectly suggests that the Ag doped Bi-MnOx could be more active for possible visible light photo catalytic applications.

The silver nanoparticle has been shown to exhibit interesting electro catalytic and bio sensing properties in various applications [37–39]. High surface-to-volume ratio and particle size of AgNPs allow them to interact with microbial membranes of different pathogens. The antibacterial property of silver nanoparticle is exploited for many applications in a wide range of fields, including medicine and dentistry [40]. Hence, the as-prepared silver nanoparticle with quantum dot size is an active substance to exploit the antibacterial property against the bacterial strains. Hence, in the present work, the silver nanoparticle and graphene oxide modified Bi-MnOx materials are analyzed for possible antimicrobial property against various strains of bacterial pathogens. The concentration of Ag@Bi-MnOx addition in the cultured plate was maintained between 50 µg and 100 µg. The schematic bar diagram of the overall order of antibacterial activity demonstrated by AgNPs and Ag nanoparticle deposited Bi-MnOx are showing in Fig. 11(a–c). The activity order of the above materials is following the trend for various gram-positive and gram-negative bacteria as follows: *Salmonella typhi(-) > Streptococcus mutants(+)> Escherichia coli (-)> Staphylococcus aureus(+)~ P.aeruginosa (-)*. Silver nanoparticle alone is showing higher activity and sensitivity towards both types of bacterial strains. In the case of Ag nanoparticle doped Bi-MnOx showing antibacterial activity with a concentration range of 50 and 100 µg, the low concentration of Ag@Bi-MnOx is not showing any sensitivity at a lower concentration of Ag@Bi-MnOx addition in a culture plate. The silver nanoparticle and graphene oxide modified Bi-MnOx shows the enhanced antimicrobial activity (Fig. 11c) compared to Ag@Bi-MnOx. Figure 11(d) showing the Mueller-Hinton agar plates of Ag nanoparticle activity for bacterial strain damage in the culture plates. Even, very low concentration (1 µg) of silver nanoparticle are showing effective antibacterial activity (Fig. 11d). Hence, the purpose of silver nanoparticle deposition on Bi-MnOx for antimicrobial activity to implement large scale production of a low cost method prepared Ag and GO modified Bi-MnOx composite towards smart health care building formation, ceramic tiles fabrication for prevent the antimicrobial infections in health care sector.

4 Conclusion

Ultra-sonication assisted fabrication of silver and silver-reduced graphene oxide incorporation on Bi-MnOx nanotube composite have successfully prepared by two-stage process. The α- phase of manganese oxide and Bi_2O_3 crystalline phase are obtained as the main phase formation for the synthesized Ag deposited Bi-MnOx and silver/r-graphene oxide modified Bi-MnOx nanocomposite. Silver nanoparticle and silver/graphene oxide modified Bi-MnOx nanotubes was showing good electrochemical sensor activity towards hydrogen peroxide detection with good cyclic stability. The reduced band gap values has obtained for Ag/GO doped Bi-MnOx compared to pristine Bi-MnOx nanotubes. Silver nanoparticle modified Bi-MnOx shows efficient antibacterial activity compared to bulk Bi-MnOx. The large-scale synthesis of silver quantum dot and GO decorated Bi-MnOx could be utilized in ceramic tiles fixation and floorings in smart building construction to prevent bacterial and viral infections in healthcare sector.

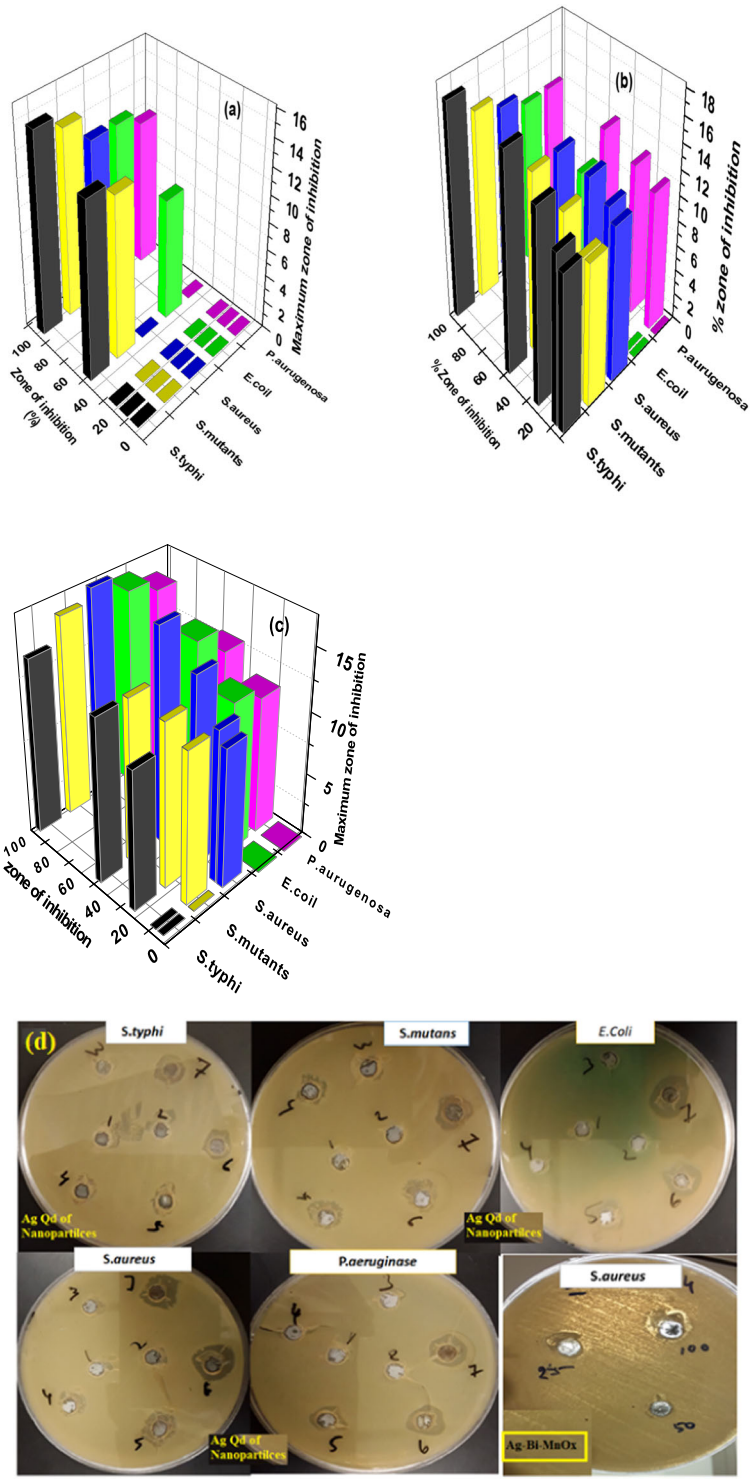

Fig. 11 Bar diagram of Antibacterial activity (**a**) -Ag@ BiMnOx (**b**) pristine Ag Quantum dot particles synthesized by biogenic method (**c**) Ag QD – graphene oxide deposited Bi-MnOx at various concentration from 5 to 100 µg (1–5) in presence of bacterial strains (**d**) Growth image of bacterial strain on as prepared Ag nanoparticle modified Bi-MnOx Nanotubes

Acknowledgements We extend their appreciation to the Deputyship for Research & Innovation, "Ministry of Education" in Saudi Arabia for funding this research work through the project no. (IFKSURG-1440-014).

Authors Contribution RJR: Supervision, Methodology; PA: Data curation, Formal analysis. HAA: Formal analysis, editing. TR: editing, Data curation, Formal analysis. AJN: Methodology, Conceptualization,. TP: analysis, writing, editing; MD W: Data collection, Methodology.

Compliance with ethical standards

Conflict of interest The authors declare that they have no conflict of interest.

References

1. Yang S, Liu L, Wang G et al. (2015) One-pot synthesis of Mn_3O_4 nanoparticles decorated with nitrogen-doped reduced graphene oxide for sensitive nonenzymatic glucose sensing. JEAC 755:15–21. https://doi.org/10.1016/j.jelechem.2015.07.021
2. Abecassis-Wolfovich M, Jothiramalingam R, Landau MV et al. (2005) Cerium incorporated ordered manganese oxide OMS-2 materials: Improved catalysts for wet oxidation of phenol compounds. Appl Catal B Environ 59:91–98. https://doi.org/10.1016/j.apcatb.2005.01.001
3. Gnana kumar G, Awan Z, Suk Nahm K, Stanley Xavier J (2014) Nanotubular MnO_2/graphene oxide composites for the application of open air-breathing cathode microbial fuel cells. Biosens Bioelectron 53:528–534. https://doi.org/10.1016/j.bios.2013.10.012
4. Rather SU (2019) Hydrogen uptake of manganese oxide-multiwalled carbon nanotube composites. Int J Hydrog Energy 325–331. https://doi.org/10.1016/j.ijhydene.2018.03.009
5. Da Costa-Serra JF, Chica A (2018) Catalysts based on Co-Birnessite and Co-Todorokite for the efficient production of hydrogen by ethanol steam reforming. Int J Hydrog Energy 43:16859–16865. https://doi.org/10.1016/j.ijhydene.2017.12.114
6. Wang Y, Bai W, Nie F, Zheng J (2015) A non-enzymatic glucose sensor based on Ni/MnO_2 nanocomposite modified glassy carbon electrode. 2399–2405. https://doi.org/10.1002/elan.201500049
7. Tang C, Zhang Y, Han J, et al. (2020) Monitoring graphene oxide's efficiency for removing Re(VII) and Cr(VI) with fluorescent silica hydrogels. Environ Pollut 262:. https://doi.org/10.1016/j.envpol.2020.114246
8. Wilk ŁJ, Ciechanowska A, Kociołek-Balawejder E (2020) Removal of sulfides from water using a hybrid ion exchanger containing manganese(IV) oxide. Sep Purif Technol 231. https://doi.org/10.1016/j.seppur.2019.115882
9. Zhou H, Xu J, Lv S, et al. (2020) Removal of cadmium in contaminated kaolin by new-style electrokinetic remediation using array electrodes coupled with permeable reactive barrier. Sep Purif Technol 239: https://doi.org/10.1016/j.seppur.2020.116544
10. Dung NT, Thu TV, Van Nguyen T et al. (2020) Catalytic activation of peroxymonosulfate with manganese cobaltite nanoparticles for the degradation of organic dyes. RSC Adv 10:3775–3788. https://doi.org/10.1039/c9ra10169a
11. Ding B, Zheng P, Ma P, Lin J (2020) Manganese oxide nanomaterials: synthesis, properties, and theranostic applications. Adv Mater 32: https://doi.org/10.1002/adma.201905823
12. Asif M, Aziz A, Quang A et al. (2015) Analytica chimica acta real-time tracking of hydrogen peroxide secreted by live cells using MnO_2 nanoparticles intercalated layered doubled hydroxide nanohybrids. Anal Chim Acta 898:34–41. https://doi.org/10.1016/j.aca.2015.09.053
13. Shypunov I, Kongi N, Kozlova J et al. (2015) Enhanced oxygen reduction reaction activity with electrodeposited Ag on manganese oxide–graphene supported electrocatalyst. Electrocatalysis 6:465–471. https://doi.org/10.1007/s12678-015-0266-x
14. Lv Q, Sun H, Li X et al. (2016) Ultrahigh capacitive performance of three-dimensional electrode nanomaterials based on α-MnO_2 nanocrystallines induced by doping Au through Å-scale channels. Nano Energy 21:39–50. https://doi.org/10.1016/j.nanoen.2015.11.009
15. Bahloul A, Nessark B, Briot E et al. (2013) Polypyrrole-covered MnO_2 as electrode material for supercapacitor. J Power Sources 240:267–272. https://doi.org/10.1016/j.jpowsour.2013.04.013
16. Hoseinpour V, Ghaemi N (2018) Green synthesis of manganese nanoparticles: applications and future perspective–A review. J Photochem Photobio B Biol 189:234–243. https://doi.org/10.1016/j.jphotobiol.2018.10.022
17. Jadhav S, Kalubarme RS, Terashima C et al. (2019) Manganese dioxide/reduced graphene oxide composite an electrode material for high-performance solid state supercapacitor. Electrochim Acta 299:34–44. https://doi.org/10.1016/j.electacta.2018.12.182
18. Liu Q, Yang J, Luo X et al. (2020) Fabrication of a fibrous MnO_2@MXene/CNT electrode for high-performance flexible supercapacitor. Ceram Int 46:11874–11881. https://doi.org/10.1016/j.ceramint.2020.01.222
19. Wang Y, Zhang D, Lu Y et al. (2019) Cable-like double-carbon layers for fast ion and electron transport: An example of CNT@NCT@MnO2 3D nanostructure for high-performance supercapacitors. Carbon NY 143:335–342. https://doi.org/10.1016/j.carbon.2018.11.034
20. Wang Q, Ma Y, Liang X et al. (2019) Flexible supercapacitors based on carbon nanotube-MnO2 nanocomposite film electrode. Chem Eng J 371:145–153. https://doi.org/10.1016/j.cej.2019.04.021
21. Ivanova AS, Slavinskaya EM, Mokrinskii VV et al. (2004) The role of support in formation of the manganese-bismuth oxide catalyst for synthesis of nitrous oxide through oxidation of ammonia with oxygen. J Catal 221:213–224. https://doi.org/10.1016/j.jcat.2003.06.001
22. Baidikova I, Matralis H, Naud J et al. (1992) Characterization of bismuth-manganese oxide catalysts for methane oxidative coupling. Appl Catal A, Gen 89:169–182. https://doi.org/10.1016/0926-860X(92)80231-Z
23. Minakshi M, Mitchell DRG (2008) The influence of bismuth oxide doping on the rechargeability of aqueous cells using MnO_2 cathode and LiOH electrolyte. Electrochim Acta 53:6323–6327. https://doi.org/10.1016/j.electacta.2008.04.013
24. Zhu Q, Liu K, Zhou J et al. (2017) Design of a unique 3D-nanostructure to make MnO_2 work as supercapacitor material in acid environment. Chem Eng J 321:554–563. https://doi.org/10.1016/j.cej.2017.03.147
25. Thiagarajan S, Tsai TH, Chen SM (2011) Electrochemical fabrication of nano manganese oxide modified electrode for the detection of H_2O_2. Int J Electrochem Sci 6:2235–2245
26. Daivajna MD, Kumar N, Gahtori B et al. (2014) Electrical conduction and thermal properties of Bi-doped Pr 0·7Sr0·3MnO_3 manganite. Bull Mater Sci 37:47–51. https://doi.org/10.1007/s12034-014-0624-y
27. Daivajna MD, Kumar N, Awana VPS et al. (2014) Electrical, magnetic and thermal properties of Pr0.6-xBixSr0.4MnO_3 manganites. J Alloy Compd 588:406–412. https://doi.org/10.1016/j.jallcom.2013.11.033
28. Ramalingam J, Vaali-Mohammed MA, Al-Lohedan HA, Appaturi JN (2017) Synthesis and bio-physical characterization of Silver nanoparticle and Ag-mesoporous MnO_2 nanocomposite for antimicrobial and anti-cancer activity. J Mol Liq. https://doi.org/10.1016/j.molliq.2017.08.037
29. Jayaprakash N, Vijaya JJ, Kaviyarasu K, et al. (2017) Green synthesis of Ag nanoparticles using Tamarind fruit extract for the antibacterial studies. J Photochem Photobiol B Biol. https://doi.org/10.1016/j.jphotobiol.2017.03.013
30. Ramalingam J, Munusamy MA, Al-lohedan HA(2016) Preparation, textural and photoluminescence characterization of green fluorescence protein-immobilised Ga-ZnO (GZO) -nanocomposites J Photochem Photobiol B: Biol 165:202–212. https://doi.org/10.1016/j.jphotobiol.2016.10.028
31. Zhang X, Chen C, Chen X et al. (2019) Ruthenium oxide modified alpha-manganese dioxide nanotube as efficient bifunctional cathode catalysts for lithium oxygen batteries. ChemistrySelect 4:7455–7462. https://doi.org/10.1002/slct.201901744

32. Ray C, Dutta S, Roy A et al. (2016) Redox mediated synthesis of hierarchical Bi_2O_3/MnO_2 nanoflowers: a non-enzymatic hydrogen peroxide electrochemical sensor. Dalt Trans 45:4780–4790. https://doi.org/10.1039/c6dt00062b
33. Vilas Bôas N, Souza Junior JB, Varanda LC et al. (2019) Bismuth and cerium doped cryptomelane-type manganese dioxide nanorods as bifunctional catalysts for rechargeable alkaline metal-air batteries. Appl Catal B Environ 258:118014
34. Chen R, Yu J, Xiao W (2013) Hierarchically porous MnO_2 microspheres with enhanced adsorption performance. J Mater Chem A 1:11682–11690. https://doi.org/10.1039/c3ta12589k
35. Li L, Du Z, Liu S et al. (2010) A novel nonenzymatic hydrogen peroxide sensor based on MnO 2/graphene oxide nanocomposite. Talanta 82:1637–1641. https://doi.org/10.1016/j.talanta.2010.07.020
36. Pal U (2007) Use of diffuse reflectance spectroscopy for optical characterization of un-supported nanostructures. Rev Mex de F'is 53:18–22
37. Ranoszek-Soliwoda K, Tomaszewska E, Małek K et al. (2019) The synthesis of monodisperse silver nanoparticles with plant extracts. Colloids Surf B Biointerfaces 177:19–24. https://doi.org/10.1016/j.colsurfb.2019.01.037
38. Judith Vijaya J, Jayaprakash N, Kombaiah K, et al. (2017) Bioreduction potentials of dried root of Zingiber officinale for a simple green synthesis of silver nanoparticles: Antibacterial studies. J Photochem Photobiol B Biol. https://doi.org/10.1016/j.jphotobiol.2017.10.007
39. Palakurthy S, P AA, K VR (2019) In vitro evaluation of silver doped wollastonite synthesized from natural waste for biomedical applications. Ceram Int 45:25044–25051. https://doi.org/10.1016/j.ceramint.2019.03.169
40. Zhang X-F, Liu Z-G, Shen W, Gurunathan S (2016) Silver nanoparticles: synthesis, characterization, properties, applications, and therapeutic approaches. Int J Mol Sci 17. https://doi.org/10.3390/ijms17091534

5 Affiliations

Jothi Ramalingam Rajabathar[1] · Prabhakarn Arunachalam[1] · Hamad A. AL-Lohedan[2] · Radhika Thankappan[3] · Jimmy Nelson Appaturi[4] · Thiruchelvi Pulingam[5] · Wasmiah Mohammed Dahan[1]

[1] Chemistry Department, College of Science, King Saud University, P.O. Box 2455, Riyadh 11451, Saudi Arabia

[2] Surfactant Research Chair, Chemistry Department, College of Science, King Saud university, Riyadh 11451, Saudi Arabia

[3] Centre for Materials for Electronics Technology [C-MET], M.G. Kavu, Thrissur, Kerala 680581, India

[4] School of Chemical Sciences, Universiti Sains Malaysia, Penang 11800, Malaysia

[5] School of Biological Sciences, Universiti Sains Malaysia, Penang 11800, Malaysia